Journal of Materials Science and Engineering B 4 (6) (2014) 163-170

XRD and XPS Analysis of TiO_2 Thin Films Annealed in Different Environments

Tamara Potlog[1], Petru Dumitriu[1], Marius Dobromir[2] and Dumitru Luca[2]

1. Department of Physics and Engineering, Moldova State University, MD 2009, Chisinau Moldova

2. Faculty of Physics, Alexandru Ioan Cuza University, Iasi 700506, Romania

Received: June 18, 2014 / Accepted: June 23, 2014 / Published: June 25, 2014.

Abstract: Undoped and Nb-doped TiO_2 thin films have been fabricated on glass substrate by RF magnetron sputtering. The morphologic, structural and surface composition of these films before and after annealing in different environments were investigated by atomic force microscopy (AFM) imaging, X-ray diffraction (XRD) and X-ray photoelectron spectroscopy (XPS). The XRD data reveal that the crystallinity is improved when the films are Nb-doped and annealed in H_2 environment. The TiO_2 thin films annealed in H_2 environment exhibit only the anatase phase. The XPS analysis of TiO_2 with Nb indicates the maximum shift in binding energy of the Ti 2p peak. A mechanism for the incorporation of Nb in the TiO_2 lattice has been proposed.

Key words: TiO_2 thin films, doping effect, H_2 annealing, XRD, XPS analysis.

1. Introduction

TiO_2 is a large bandgap semiconductor, commonly investigated more in rutile and anatase phases, has been extensively studied worldwide. Its response to UV light has led to the emergence of the photocatalysis research field [1-3]. New opportunities for the applications of the TiO_2 materials lie nowadays in more challenging areas, such as energy conversion and storage. Mesoscopic TiO_2 film is a major component of dye-sensitized solar cells [4, 5], organic photovoltaics [6] and quantum dot sensitized solar cells [7, 8]. Furubayashi et al. recently reported that Nb-doped TiO_2 could be used as a new transparent conducting oxide (TCO) material [9]. The incorporation of Nb metal ion in TiO_2 lattice acts as a donor type impurity and leads to a decrease in the resistivity of the semiconductor [10], which is critical for window layer in the fabrication of the photovoltaic devices based on hetero-junctions. In order to extend the light absorption spectrum into visible region in solar cells, we try to modify the properties of some TiO_2 films by using the Nb_2O_5 as dopant. In this paper we report the effect of annealing in different media on the structural properties and composition of the films by XRD and XPS and the mechanism for the incorporation of Nb in the TiO_2 lattice.

Corresponding author: Tamara Potlog, Ph.D., professor, research fields: TCO thin films, semiconductor materials and structure. E-mail: tpotlog@gmail.com.

2. Experiments

TiO_2 thin films were prepared on glass substrates by radio frequency (RF) magnetron sputtering of a Ti target of 99.5% purity, 76.2 mm in diameter. Additionally, TiO_2 thin films doped with oxide powder Nb_2O_5 of 99.999% purity were prepared. The sputtering was performed under a mixture of 5 standard cubic centimeters per minute (sccm) of Ar (99.99%) and 1 sccm of O_2 (99.99%) atmosphere supplied as working and reactive gases, respectively, through independent mass-flow controllers. The sputtering chamber was evacuated down to 1×10^{-5} mbar by the turbo molecular pump and the working pressure was kept at about 5×10^{-3} mbar.

During the depositions, the RF power was 100 W and the substrates were kept at room temperature using the same deposition time of 8 h. The distance between the target and the substrate was kept constant at 6 cm. Before the deposition, the glass substrates were sequentially cleaned in an ultrasonic bath with acetone then ethanol. Finally, the substrates were rinsed with distilled water and dried. After the deposition, the undoped and Nb-doped TiO_2 films were vacuum-annealed in hydrogen environment. The first set of undoped TiO_2 films was vacuum-annealed at 420 °C for 30 min in the deposition chamber at a pressure of 4.0×10^{-5} mbar and in hydrogen atmosphere at a pressure of 2.0×10^{-3} mbar. A second set of Nb-doped TiO_2 films was annealed at 420 °C for 30 min in hydrogen atmosphere at the same pressure, as the first set. We denote the first set of pristine TiO_2 films as MD-2 and the second one as TiNbO-2.

The crystal structure was studied by X-ray diffraction (XRD) using a Bruker-AXS, D8 Advance diffractometer (CuK_α radiation, 40 mA, 40 kV). The weight percentage of the anatase phase (W_A) was calculated with the relation [11]:

$$W_A = \frac{1}{1 + 1.265\, I_R / I_A} \quad (1)$$

where, I_A denotes the intensity of the strongest anatase reflection and I_R is the intensity of the strongest rutile reflection.

The elemental composition in the surface region was investigated by X-ray photoelectron spectroscopy (XPS). The spectra were measured using a Physical Electronics PHI 5000 Versa Probe instrument, equipped with a monochromated AlK_α X-ray source (1,486.6 eV). The photoelectrons were collected at a take-off angle of 45°. The surface quantification was done following the standard procedure [12] using the Ti 2p, O 1s, and Nb 3d high-resolution XPS spectra. Peak deconvolution has been done using the PHI-MULTIPAK software. The elemental atomic concentration was calculated from the peak surface areas, taking into account the sensitivity factors of the analyzed elements[13].

3. Results and Discussion

3.1 Morphological and Structural Studies of TiO_2 Thin Films

The diffraction pattern for the first set of undoped TiO_2 films is shown in Fig. 1. The various diffraction peaks could be assigned to reflections corresponding to the anatase and rutile phases of TiO_2 [14] for the as-deposited and the vacuum-annealed films. For the as-deposited TiO_2 film, the weight percentage of the anatase phase (W_A) is 59.3%. For the vacuum-annealed film the weight percentage of the anatase phase (W_A) increases to 62%. The TiO_2 films annealed in H_2 atmosphere exhibit only the anatase phase.

The diffraction spectra of the second set of Nb-doped TiO_2 films are depicted in Fig. 2. The XRD data show that the crystallinity is improved when the films are doped.

Annealing at 420 °C in H_2 atmosphere results in an increase in the intensity of the diffraction peak located at $2\theta = 25.2°$. No characteristic peaks of Nb_2O_5 were observed in Nb-doped TiO_2 thin films. Instead, it is found that the peak position of (101) anatase plane shifts to smaller diffraction angle values. This may ascribed to the exchange of Nb with Ti in the TiO_2 lattice [15] and the formation of the TiNbO phase with different concentrations.

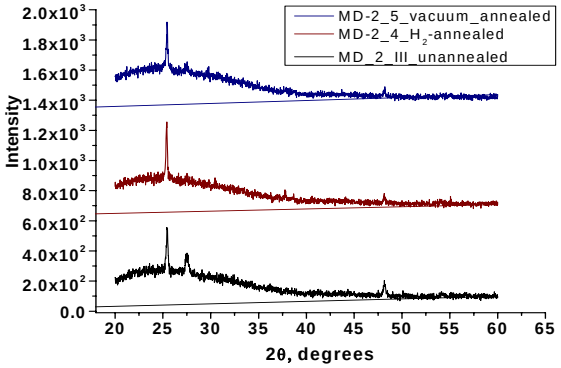

Fig. 1 The XRD patterns of the as-deposited, vacuum-annealed and hydrogen-annealed TiO_2 films. The annealing temperature was 420 °C (see text).

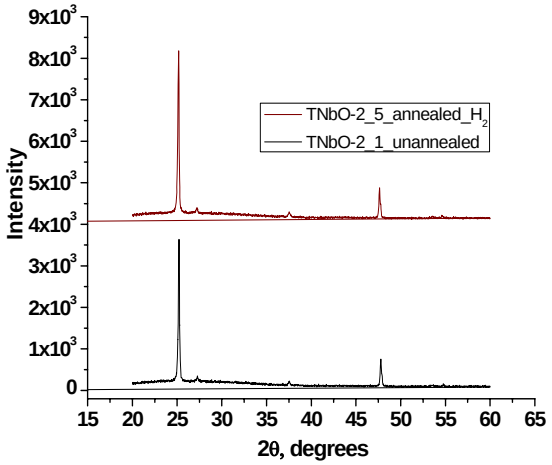

Fig. 2 XRD patterns of the $NbTiO_2$ film in the as-deposited and annealed in H_2 states. .

This fact was confirmed by the analysis with the TOPAS-Academic V5 software. The weight percentage of the anatase phase (W_A) is 93% for annealed Nb-doped TiO_2 film, while for the unannealed it is 96%. The *a* and *c* lattice parameters of the TiO_2 crystalline cell decrease from (a = 3.8214 Å, c = 9.5868 Å) to (a = 3. 7842 Å, c = 9.5185 Å), respectively. This is caused by the differences in Nb concentration, as confirmed below by the XPS analysis (Table 2).

We suppose that the primary hydrogen annealing mechanism is the chemisorption of the dissociated hydrogen on the surface of the films. The half width of all the peaks of the Nb-doped and annealed TiO_2 thin films increases. The crystallite size was calculated by Scherer equation using anatase (101) and (110) rutile phases. As shown in Table 1, for samples annealed in H_2 atmosphere at 420 °C the estimated crystallite size for the anatase phase increases for both sets.

Figs. 3 and 4 show the AFM images of Nb-doped TiO_2 films as-grown at room temperature and annealed at 420 °C for 30 min in hydrogen atmosphere. The AFM measurements reveal a net discrepancy and indicate an increase of crystallinity of the annealed films. The as-deposited TiO_2 film exhibits a smooth surface_with non-uniform grains. After annealing, the surface becomes homogeneous and is composed of many nanocrystalline grains.

3.2 X-Ray Photoelectron Spectroscopy Analysis

Fig. 5 shows the survey XPS spectra of the first set of TiO_2 films in the whole binding energy region. The characteristic peaks of C 1s, O 1s and Ti 2p are present.

Table 1 Structural parameters of TiO_2 thin films.

Sample	2θ	Intensity (arb. units)	Phase name	d (Å)	D (nm)
MD-2_5 (unannealed)	25.508	601*	(101) Anatase	1.7954	51.0 44.1
	27.438	283	(110) Rutile	3.3228	
	48.042	170	(200) Anatase	3.1042	
MD-2_1 (vacuum, 420 °C)	25.503	556*	(101) Anatase	1.7967	51.5
	27.438	386	(110) Rutile	3.3304	
	48.043	204	(200) Anatase	3.1003	
MD-2_4 (H_2, 420 °C)	25.508	636*	(101) Anatase	1.7981	88.4
	37.793	186	(004) Anatase	2.5118	
	48.048	162	(200) Anatase	3.1064	
TiNbO_2_1 (unannealed)	25.192	3643*	(101) Anatase	1.8121	47.4
	27.432	246	(110) Rutile	3.3591	
	37.789	156	(004) Anatase	3.7975	
	47.783	749	(200) Anatase	4.1726	
TiNbO_2_5 (H_2, 420 °C)	25.162	4126*	(101) Anatase	1.8141	55.2
	27.420	226	(110) Rutile	3.3738	
	37.792	207	(004) Anatase	3.7975	
	47.747	827	(200) Anatase	4.1783	

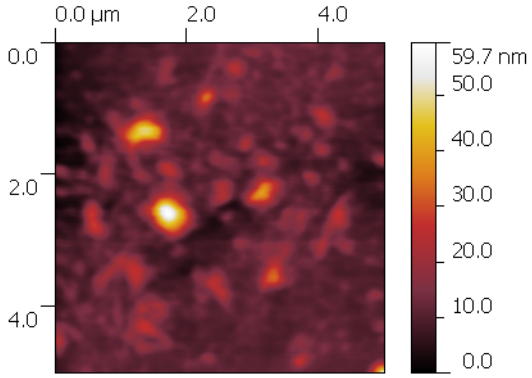

Fig. 3 Two-dimensional AFM image of an as-grown Nb-doped TiO_2 thin film.

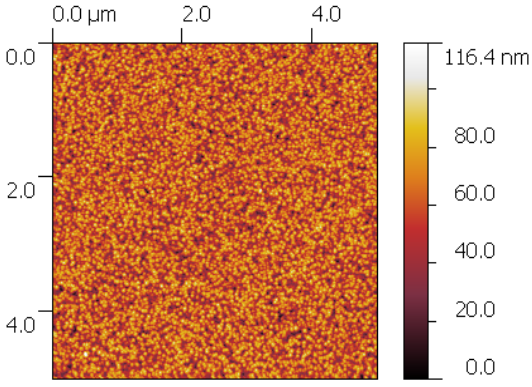

Fig. 4 Two-dimensional AFM images of a Nb-doped TiO_2 thin film annealed in H_2 atmosphere at 420 °C.

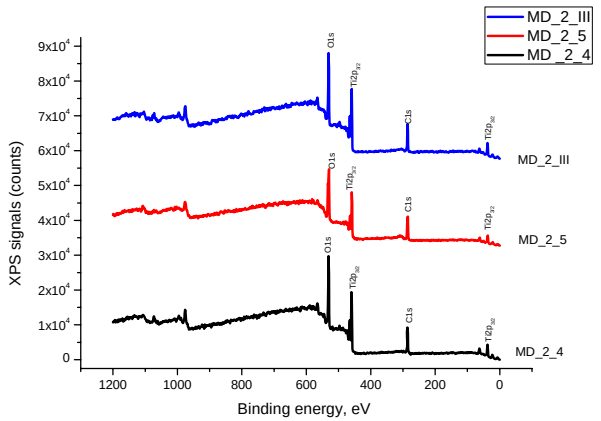

Fig. 5 XPS survey scan spectra of an as-deposited TiO_2 film, vacuum-annealed and annealed in H_2 atmosphere at 420 °C.

The C 1s peak of the unannealed film is located at a binding energy value of 284.6 eV, while for the sample annealed in H_2 it shifts to 285.7 eV.

Fig. 6 shows the high-resolution Ti 2p doublet of the pristine TiO_2 films. For the unannealed TiO_2 film the spectrum indicates binding energies at 458.5 ± 0.2 eV for Ti $2p_{3/2}$ and 464.3 ± 0.2 eV for Ti $2p_{1/2}$, respectively, which are very close to the values of the Ti^{4+} valence state of stoichiometric rutile TiO_2 [16, 17].

For the vacuum and H_2 annealed films at 420 °C the binding energies of the Ti 2p feature binding energy values shifted towards 459.5 ± 0.2 eV for Ti $2p_{3/2}$ and 465.2 ± 0.2 eV for Ti $2p_{1/2}$, also reported in Ref. [18]. We suppose that this shift could be generated by the reduction of Ti^{4+} ions to Ti^{3+} defect states which usually are accompanied by a loss of oxygen from the surface of TiO_2.

Liu et al. [19] proposed that the interaction between H_2 and TiO_2 fell develops in three successive steps. Firstly, hydrogen interacts physically with the adsorbed oxygen on the surface of TiO_2. Secondly, electrons are transferred from the H to the O atoms in the lattice of TiO_2. Then, the oxygen vacancies are formed when the O atom and the H atom form of H_2O or OH groups. Thirdly, when the temperature increased to 420 °C, the interaction between H_2 and TiO_2 proceeds more drastically, the electrons are transferred from oxygen vacancies to Ti^{4+} ions, and then Ti^{3+} defect states are formed. Zhang et al. [20] irradiated the TiO_2/Si films by electron beams and found that the number of Ti^{3+} ions increased and Ti^{4+} ions decreased after the irradiation. The atomic concentration of Ti and

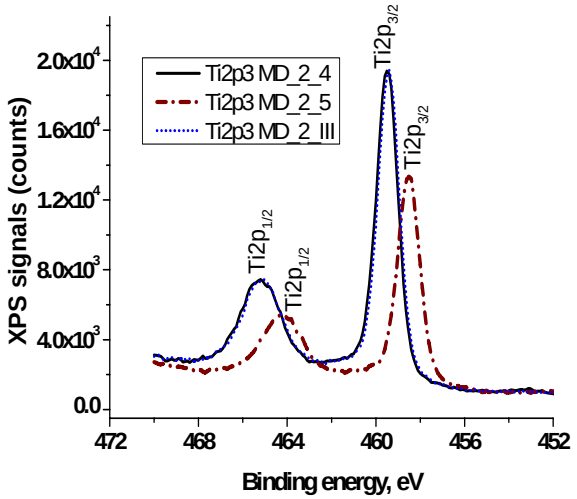

Fig. 6 XPS spectra of Ti2p region of an as-deposited TiO_2 film, vacuum-annealed and annealed in H_2 atmosphere at 420 °C.

Table 2 The atomic concentration and the binding energies for the Ti 2p, Nb 3d and O 1s lines.

Samples	XPS Peak	%	XPS Peak	%
MD_2_4 (H_2, 420 °C)	O 1s	38.1	O 1s	60.1
	C 1s	36.7	Ti $2p_{3/2}$	39.9
	Ti 2p	25.3		
MD_2_5 (unannealed)	O 1s	42.8	O 1s	74.0
	C 1s	42.2		
	Ti $2p_{3/2}$	15.0	Ti $2p_{3/2}$	26.0
MD_2_I (vacuum, 420 °C)	O 1s	38.1	O 1s	61.5
	C 1s	38.0		
	Ti $2p_{3/2}$	23.8	Ti $2p_{3/2}$	38.5
TiNbO_2_1 (unannealed)	O 1s	41.3	O 1s	61.6
	C 1s	32.9		
	Ti $2p_{3/2}$	21.5	Ti $2p_{3/2}$	32.0
	Nb 3d	4.3	Nb 3d	6.4
TiNbO_2_5 (H_2, 420 °C)	O 1s	41.5	O 1s	59.8
	C 1s	30.5		
	Ti $2p_{3/2}$	22.1	Ti $2p_{3/2}$	31.9
	Nb 3d	5.8	Nb 3d	8.3

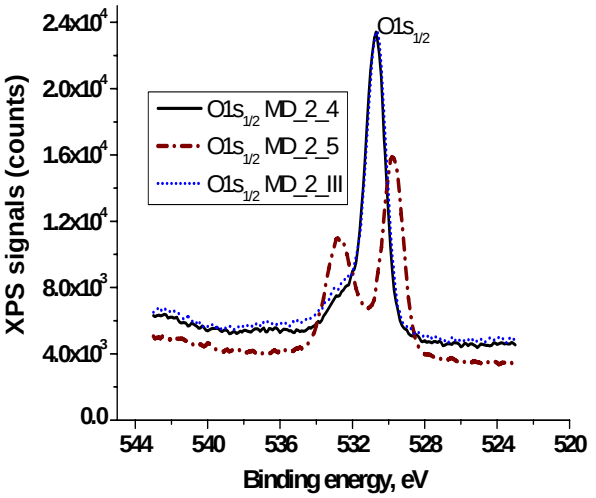

Fig. 7 XPS spectra of O1s region of as-deposited TiO_2 film, vacuum-annealed and annealed in H_2.

O in the TiO_2 thin films are shown in Table 2.

We can conclude that the Ti^{4+} ions are reduced by both electron donors such as H_2 and lattice oxygen in TiO_2 and the binding energy of 459.5 eV may be attributed in this case to Ti^{3+} defect state of anatase TiO_2 phase, according to the XRD analysis. Significant increases in the intensity of the Ti 2p peaks are observed, too.

Fig. 7 shows high-resolution O 1s XPS spectrum. For the unannealed TiO_2 film, two oxygen chemical species appear, the lower binding energy (BE) at around 529.7 ± 0.2 eV can be attributed to the basic peak of TiO_2 lattice oxygen (O_{lat}); the other 532. 8 ± 0.2 eV represented the surface weakly bound (or adsorbed) oxygen (OH and molecular O_2 species). The O 1s spectrum of the vacuum-- and H_2- annealed films at 420 °C consists of a main peak with higher intensity at about 530.7 ± 0.2 eV and an obvious shoulder located at about 532.9 ± 0.2 eV, indicating that the detected OH group and molecular O_2 may be adsorbed at the surface of the film during annealing. The binding energies of the O 1s signal of the vacuum- and H_2- annealed films shifted toward higher binding energies with the same value 1.0 ± 0.2 eV as for Ti 2p spectrum of these films.

Figs. 8-10 depict the high-resolution Nb 3d, Ti 2p and O 1s signals of the unannealed Nb-doped TiO_2 films and annealed in H_2 atmosphere at 420 °C, respectively. From Table 2 it can be observed that the atomic percentage of the Nb element is different in unannealed TiO_2 films, compared to the films after H_2 annealing. Therefore, for these samples it is hard to discuss about the influence of the H_2 treatment on their structural properties. The Nb 3d binding energy for the unannealed Nb-doped TiO_2 film was determined to be 208.2 ± 0.2 eV for Nb $3d_{5/2}$ and 211.0 ± 0.2 eV for Nb $3d_{3/2}$, while for the annealed one in hydrogen, the BE

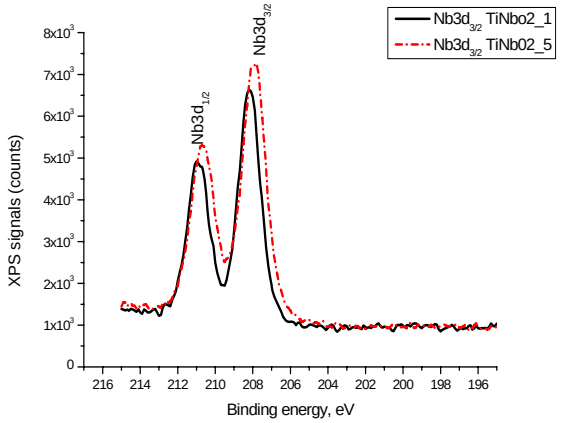

Fig. 8 XPS spectra of Nb3d region of an as-deposited Nb doped TiO_2 film and annealed in H_2.

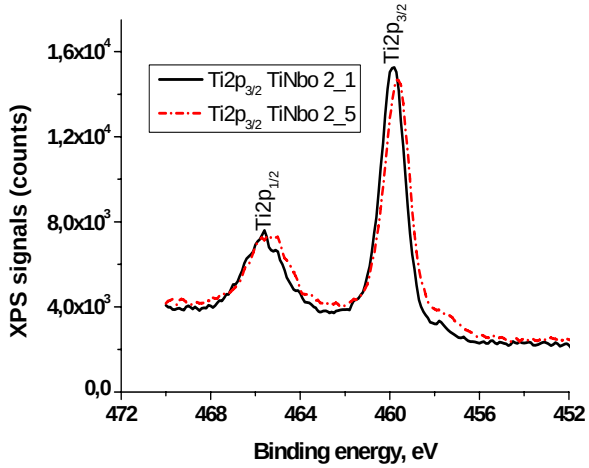

Fig. 9 XPS spectra of Ti 2p region of unannealed and annealed Nb-doped TiO_2 films.

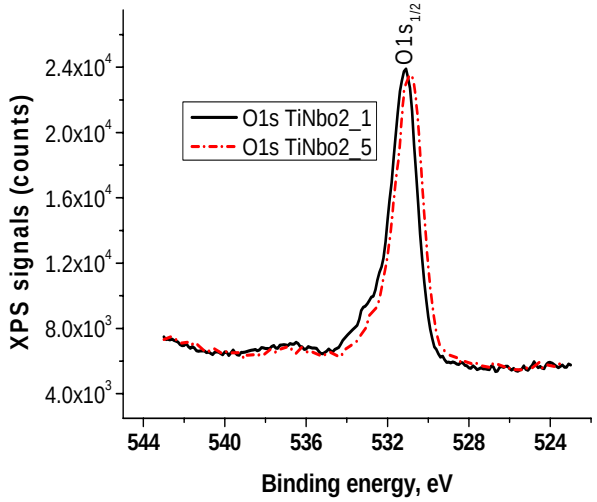

Fig. 10 XPS spectra of O1s region of unannealed and annealed Nb-doped TiO_2 films.

values are is 207.9 ± 0.2 eV and 210.8 ± 0.2 eV, respectively.

We suppose that this shift are caused by the differences in atomic concentration of Nb (Table 2) and by the effect of annealing in H_2 atmosphere..

The Ti 2p XPS spectra (Fig. 9) of unannealed Nb-doped TiO_2 films show values of binding energies of 459.7 ± 0.2 eV for Ti $2p_{3/2}$ and 464.9 ± 0.2 eV for Ti $2p_{1/2}$, respectively.

For the film annealed in H_2 atmosphere, a slight shift (~ 0.2 eV) towards higher BE values is seen for Ti $2p_{3/2}$ and (~ 0.6 eV) for Ti $2p_{1/2}$. The position of the Ti $2p_{3/2}$ peak (458.8 eV) is close to the value reported for Ti^{3+} states in the anatase phase (458.7 eV) [21]. We believe that the H_2 annealing changes the Ti^{3+}/Ti^{4+} ratio in the TiO_2 thin film. Both $2p_{1/2}$ and $2p_{3/2}$ binding energies showed a change in Ti^{3+} states and the Ti^{4+} ions, as a consequence of the H_2 treatment.

A chemical shift of the BE is known to mean changes in the structure. Since the ionic radius of Nb^{5+} (0.70 Å) is larger than the ionic radius (0.68 Å) of the titanium, we can thus conclude that the Nb is easily built into a lattice, adding electrons. The theoretical calculations of Morgan [22] predict a small-polaronic Ti^{3+}gap state within an Nb-doped TiO_2 thin film. For Nb dopant at these concentrations, the defect can be characterized as Nb^{5+} and Ti^{3+}/Ti^{4+} ratio.

The peak of the Nb $3d_{3/2}$ peak corresponds to that of Nb^{5+} oxidation state [23, 24]. Nb^{5+} species, substituting for Ti^{4+} in the crystalline lattice could be a reason for anatase stabilization. To maintain the charge equilibrium, the extra-positive charge due to Nb^{5+} may be compensated by the creation of an equivalent amount of Ti^{3+} ions [25] or by the presence of vacancies in the cation sites [26].

The O 1s XPS spectra of the Nb-doped TiO_2 samples showed in Fig. 9 indicate that there a single chemical state. The binding energy of 531.1 ± 0.2 eV for unannealed and 530.8 ± 0.2 eV for annealed Nb-doped TiO_2 films can be attributed to surface species, such as Ti-OH resulting from the chemisorbed water (OH) [27, 28], and to the lattice oxygen (Ti-O), respectively. The shift of the binding energy to small

values for the annealed Nb-doped TiO_2 film can be attributed to the fact that a part of the OH group is adsorbed from the surface, because the weight percentage of O atoms is reduced from 61.6% to 59.8%.

4. Conclusions

Annealing in hydrogen atmosphere showed substantial improvement of structural properties TiO_2 thin films. Undoped thin films of TiO_2, are *n*-type conductors with doubly ionized oxygen vacancies as predominant point defects. The XRD data show that the crystallinity is improved when the TiO_2 films upon Nb doping. The Nb ions incorporate into the TiO_2 lattice. The XPS results indicate that the charge transfer from Nb metal ions to Ti leads to a change in the oxidation state of titanium. The H_2 annealing changes the Ti^{3+}/Ti^{4+} ratio in the TiO_2 thin film.

These results demonstrate that hydrogen annealing is a simple and effective tool to enhance and modify the properties of the original material.

Acknowledgments

This research was supported by the Bilateral Moldova-Romania grant no. 13.820.15.19/RoA.

References

[1] K. Maeda, K. Domen, Photocatalytic water splitting: Recent progress and future challenges, J. Phys. Chem. Lett. 1 (2010) 2655-2661.

[2] W.Y. Teoh, J.A. Scott, R. Amal, Progress in heterogeneous photocatalysis: From classical radical chemistry to engineering nanomaterials and solar reactors, J. Phys. Chem. Lett. 3 (2012) 629-639.

[3] P.V. Kamat, Manipulation of charge transfer across semiconductor interface, J. Phys. Chem. Lett. 3 (2012) 663-672.

[4] L.M. Peter, The Gratzel cell: Where next? J. Phys. Chem. Lett. 2 (2011) 1861-1867.

[5] T. Miyasaka, Toward printable sensitized mesoscopic solar cells: Light-harvesting management with thin TiO_2 films, J. Phys. Chem. Lett. 2 (2011) 262-269.

[6] E.L. Ratcliff, B. Zacher, N.R. Armstrong, Selective interlayers and contacts in organic photovoltaic cells, J. Phys. Chem. Lett. 2 (2011) 1337-1350.

[7] I. Mora-Sero, J. Bisquert, Breakthroughs in the development of semiconductor-sensitized solar cells, J. Phys. Chem. Lett. 1 (2010) 3046-3052.

[8] A. Braga, S. Gimenez, I. Concina, A. Vomiero, I. Mora-Sero, Panchromatic sensitized solar cells based on metal sulfide quantum dots grown directly on nanostructured TiO_2 electrodes, J. Phys. Chem. Lett. 2 (2011) 454-460.

[9] Y. Furubayashi, T. Hitosugi, Y. Yamamoto, K.Inaba, G. Kinoda, Y. Hirose, T. Shimada T. Hasegawa, A transparent metal: Nb-doped anatase TiO_2, Applied Physics Letters 86 (2005) 252101-1-252101-3.

[10] M.F. Yan, W.W. Rhodes, Effect of cation contaminants in conductive TiO_2 ceramics, J. Appl. Phys. 53 (12) (1983) 8809-8818.

[11] JCPDS X-ray powder files data (Data file 05-0522).

[12] J.F. Watts, J. Wolstenholme, An Introduction to Surface Analysis by XPS and AES, John Wiley & Sons, Chichester, 2003.

[13] J.F. Moulder, W.F. Stickle, P.E. Sobol, K.D. Bomben, Handbook of X-Ray Photolectron Spectrosopy, ULVAC-PHI Japan, Physical Electronics, USA, 1995.

[14] JCPDS Data Cards 00-021-1272 and 00-21-1276, p 521.

[15] R. Sharma, M. Bhatnagar, Improvement of the oxygen gas sensitivity in doped TiO_2 thick films Sens. Actuators B 56 (3) (1999) 215-219.

[16] H.S. Kim, S.H. Kang, Effect of hydrogen treatment on anatase TiO_2 nanotube arrays for photoelectrochemical water splitting bull, Korean Chem. Soc. 34 (7) (2013) 2067-2072.

[17] H.J. Bae, S.H. Park, A. Nakamura, K. Koike, K. Fujii, H.J. Park, et al., The effect of rapid temperature annealing with N_2 and H_2 on photoelectrochemical properties of u-TiO_2, J. Electrochem. Soc. 160 (11) (2013) H800-H802.

[18] C.D. Wagner, W.M. Riggs, L.E. Davis, J.F. Moulder, G.E. Muilenberg, Handbook of X-Ray Photoelectron Spectroscopy, Perkin Elmer Corp, Publishers, Eden Prairie, MN, 1979, p. 68.

[19] G.X. Liu, F.K. Shan, J.J. Park, W.J. Lee, G.H. Lee, I.S. Kim, et.al., Electrical properties of Ga2O3-based dielectric thin films prepared by plasma enhanced atomic layer deposition (PEALD), J Electroceram 17 (2006) 145-149.

[20] J. Zhang, Y. Wang, Z. Jin, Z. Wu, Z. Zhang, Visible-light photocatalytic behavior of two different N-doped TiO_2, Appl. Surf. Sci. 254 (2008) 4462-4466.

[21] M. Sacerdoti, M.C. Dalconi, M.C. Carotta, B. Cavicchi, M. Ferroni, S. Colonna, et al., XAS investigation of tantalum and niobium in nanostructured TiO_2 anatase, Journal of Solid State Chemistry 177 (6) (2004) 1781-1788.

[22] B.J. Morgan, D.O. Scanlon, G.W. Watson, Intrinsic n-type defect formation in TiO_2: A comparison of rutile and

anatase from GGA + U Calculations, Journal of Materials Chemistry 19 (2009) 5175-5178.

[23] M.Z. Atashbar, H.T. Sun, B. Gong, W. Wlodarski, R. Lamb, XPS study of Nb-doped oxygen sensing TiO_2 thin films prepared by sol-gel method, Thin Solid Films 326 (1-2) (1998) 238-244.

[24] J.F. Moulder, W.F. Stickle, P.E. Sool, K.D. Bomben, Handbook of X-Ray Photoelectron Spectroscopy, Perkin-Elmer Corporation, Eden Prairie, Minn, USA, 1999.

[25] M. Valigi, D. Cordischi, G. Minelli, P. Natale, P. Porta, A structural, thermogravimetric, magnetic, electron spin resonance, and optical reflectance study of the NbO_xTiO_2 system, Journal of Solid State Chemistry 77 (2) (1988) 255-263.

[26] M. Sacerdoti, M.C. Dalconi, M.C. Carotta, B. Cavicchi, M. Ferroni, S. Colonna, et al., XAS investigation of tantalum and niobium in nanostructured TiO_2 anatase, J. Solid State Chem.177 (6) (2004) 1781-1788.

[27] M. Park, T.E. Mitchell, A.H. Heuer, Subsolidus equilibria in the TiO_2 -SnO_2 system, J. Am. Ceram. Soc. 58 (1975) 43-47.

[28] J.C. Colmenares, M.A. Aramendıa, A. Marinas, J.M. Marinas, F.J. Urbano, Synthesis, characterization and photocatalytic activity of different metal-doped titania systems, Appl. Catal. A: Gen. 306 (2006) 120-127.